JACS
JOURNAL OF THE AMERICAN CHEMICAL SOCIETY
Article
pubs.acs.org/JACS

Co–Ln Mixed-Metal Phosphonate Grids and Cages as Molecular Magnetic Refrigerants

Yan-Zhen Zheng,[†,∥] Marco Evangelisti,[§] Floriana Tuna,[†] and Richard E. P. Winpenny*[,†,‡]

[†]School of Chemistry, and [‡]The Photon Science Institute, The University of Manchester, Oxford Road, M13 9PL, Manchester, United Kingdom

[§]Instituto de Ciencia de Materiales de Aragón, Departamento de Física de la Materia Condensada, CSIC-Universidad de Zaragoza, 50009, Zaragoza, Spain

[∥]Center for Applied Chemical Research, Frontier Institute of Science and Technology, Xi'an Jiaotong University, Xi'an 710054, China

Supporting Information

ABSTRACT: The synthesis, structures, and magnetic properties of six families of cobalt–lanthanide mixed-metal phosphonate complexes are reported in this Article. These six families can be divided into two structural types: grids, where the metal centers lie in a single plane, and cages. The grids include [4 × 3] $\{Co_8Ln_4\}$, [3 × 3] $\{Co_4Ln_6\}$, and [2 × 2] $\{Co_4Ln_2\}$ families and a [4 × 4] $\{Co_8Ln_8\}$ family where the central 2 × 2 square is rotated with respect to the external square. The cages include $\{Co_6Ln_8\}$ and $\{Co_8Ln_2\}$ families. Magnetic studies have been performed for these compounds, and for each family, the maximum magnetocaloric effect (MCE) has been observed for the Ln = Gd derivative, with a smaller MCE for the compounds containing magnetically anisotropic 4f-ions. The resulting entropy changes of the gadolinium derivatives are (for 3 K and 7 T) 11.8 J kg^{-1} K^{-1} for $\{Co_8Gd_2\}$; 20.0 J kg^{-1} K^{-1} for $\{Co_4Gd_2\}$; 21.1 J kg^{-1} K^{-1} for $\{Co_8Gd_4\}$; 21.4 J kg^{-1} K^{-1} for $\{Co_8Gd_8\}$; 23.6 J kg^{-1} K^{-1} for $\{Co_4Gd_6\}$; and 28.6 J kg^{-1} K^{-1} for $\{Co_6Gd_8\}$, from which we can see these values are proportional to the percentage of the gadolinium in the core.

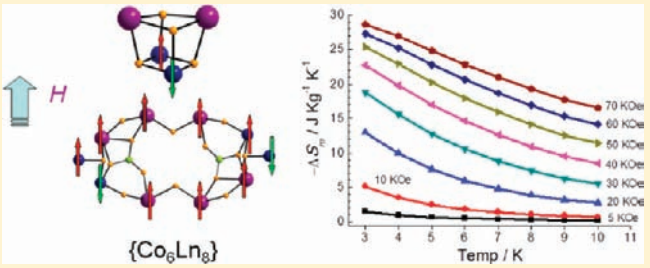

INTRODUCTION

Magnetic refrigeration is based on the magnetocaloric effect (MCE), which was first discovered in 1881 by Warbourg.[1,2] MCE is the thermal effect of magnetic materials subjected to magnetic field variation. In brief, when applying a magnetic field to a magnetic material, their magnetic moments become ordered, which reduces the total entropy of the material. In the reverse step, adiabatic demagnetization, the entropy of the magnetic material increases, and this has to be balanced by a change in the free energy of the surroundings. As a result, the system cools. Two temperature regions are particularly interesting, the near room temperature region and the ultralow temperature region (<5 K) to replace helium-3 as a coolant.

Molecular nanomagnets[3] that contain an inorganic core surrounded by organic ligands are often paramagnets down to liquid-helium temperatures. A good molecular magnetic refrigerant should have a high-spin state in a small external magnetic field and should have a small magnetic anisotropy. Recent work to make such molecular magnetic refrigerants includes $\{Fe_{14}\}$, $\{Fe_{17}\}$, $\{Mn_{10}\}$, $\{Mn_{14}\}$, $\{Mn_{17}\}$, $\{Mn_{19}\}$,$\{Mn_{32}\}$, $\{Mn_4Ln_4\}$, $\{Co_xLn_y\}$, $\{Ni_6Gd_6\}$, $\{Cu_5Gd_4\}$, $\{Gd_2\}$, and $\{Gd_7\}$ cages.[4−11] We have looked at 3d–4f mixtures for this application[11] and here report complexes involving cobalt(II) ions, which are magnetically anisotropic, with a range of lanthanide ions. Previous work on the magnetism of 3d–4f complexes began with Benelli and Gatteschi's very influential work on Cu–Gd compounds,[12] which showed that the exchange in these complexes was normally ferromagnetic. More recently, the Christou group,[13] and others,[14] have examined 3d–4f complexes as "single molecule magnets". The $\{Mn_4Ln_4\}$ complex, reported by Dalgarno et al.,[8a] is the first example of this class of compounds being used in magnetic cooling.

Here, we report studies on a range of Co–4f complexes, some of which show very large values for the MCE. By comparing a range of compounds, we show that cages containing gadolinium(III) have a larger MCE than those containing anisotropic dysprosium(III), terbium(III), holmium(III), or erbium(III) ions. The replacement of the paramagnetic lanthanides with the diamagnetic yttrium(III) ion provides information on magnetic interactions between the cobalt(II) ions.[13,14]

We have used phosphonate ligands, which show multiple coordination modes, and this combined with the variable coordination number of the cobalt(II) sites lead to a very large number of new structures. In this work, the phosphonates show five different coordination modes, which are shown in Scheme 1. Phosphonates have been used in making layered compounds[15] and more recently in making paramagnetic complexes of 3d–metals.[16] The exploitation of these ligands to make 3d–4f complexes is comparatively unusual.[17−19]

Received: September 8, 2011
Published: December 14, 2011

   dx.doi.org/10.1021/ja208367k | J. Am. Chem.Soc. 2012, 134, 1057−1065

Scheme 1. Coordination Modes of Phosphonate (a), Pivalate or Acetate (b), and Nitrate (c) in This Article, Labeled with Harris Notation[20]

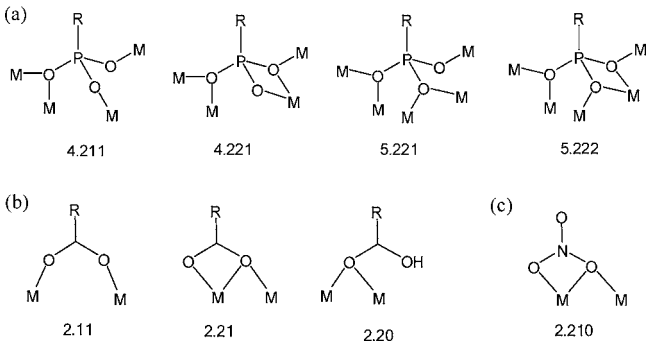

RESULTS AND DISCUSSION

Synthesis. All complexes were synthesized from the starting material $[Co^{II}_2(\mu\text{-}OH_2)(O_2C^tBu)_4]\cdot(HO_2C^tBu)_4$ **Co_2**, which was made by a literature method.[20] We have used two types of lanthanide starting materials, the hydrated lanthanide nitrate salts and dimetallic pivalate complexes $[Ln_2(O_2C^tBu)_6(HO_2C^tBu)_6]$ (Ln = Gd **Gd_2**, Tb **Tb_2**, Dy **Dy_2**, and Y **Y_2**). We have also carried out the reaction with and without additional base, and with variation of the phosphonic acid used. Through these variations, we have produced seven different structural types (Figure 1). The reactions were performed in simple autoclaves using, in general, MeCN as the solvent, and crystals were obtained either directly from cooling the solution at the end of the reaction, or by allowing the solution formed in the autoclave to stand for several days. In general, experiments with Ln heavier than Gd give crystals directly from the autoclave, while with Ln = Nd, we have only found crystals after several days. The reactions Ln−Gd gave crystals both directly and from the filtrate.

In the absence of base, the reaction of **Co_2** with a lanthanide nitrate and *tert*-butylphosphonic acid gives the first family, $[Co^{II}_8Ln^{III}_8(\mu_3\text{-}OH)_4(NO_3)_4(O_3P^tBu)_8(O_2C^tBu)_{16}]$ **1** (Ln = Gd **1Gd**, Tb **1Tb**, Dy **1Dy**, Ho **1Ho**, Er **1Er**, Yb **1Yb**, and Y **1Y**). Although the reaction is performed in mildly acidic conditions, the presence of hydroxide in the structure is not surprising because lanthanide ions can cause hydrolysis of bound water molecules even at pH 1.[21] The yield of the gadolinium complex **1Gd** is lower than for the heavier Ln ions.[11a] The compounds can be recrystallized from dichloromethane. For gadolinium, we also isolated the compound $[Co^{II}_4Gd^{III}_2(O_3P^tBu)_2(O_2C^tBu)_{10}(MeCN)_2](MeCN)_2$ **5Gd**, by allowing the clear solution obtained from the autoclave to stand at room temperature. We have also made the equivalent **5Nd** complex, which suggests that this hexametallic cage will form for the lighter lanthanides. The lower yield of **1Gd** and the isolation of a second complex for Ln = Gd and Nd suggests that the size of the lanthanide ion influences the product formed.

If a base (e.g., Et_3N, NaOMe, NaOEt, and KOH) is added to the reaction, a second family of compounds forms: $[Co^{II}_6Ln^{III}_8(\mu_3\text{-}OH)_8(O_3P^tBu)_6(O_2C^tBu)_{16}(H_2O)_2(MeCN)_x](MeCN)_y$ **4** (for $x = 0$ and $y = 2$, Ln = Gd **4Gd**, Tb **4Tb**, Dy **4Dy**, and Ho **4Ho**; for $x = 2$ and $y = 1$, Ln = Er **4Er**, Yb **4Yb**, and Y **4Y**). This reaction occurs in a range of bases and in MeCN, DMF, and toluene, which suggests this family of compounds are the strongly favored products for the heavier lanthanides. We have not obtained crystalline material from this reaction when using

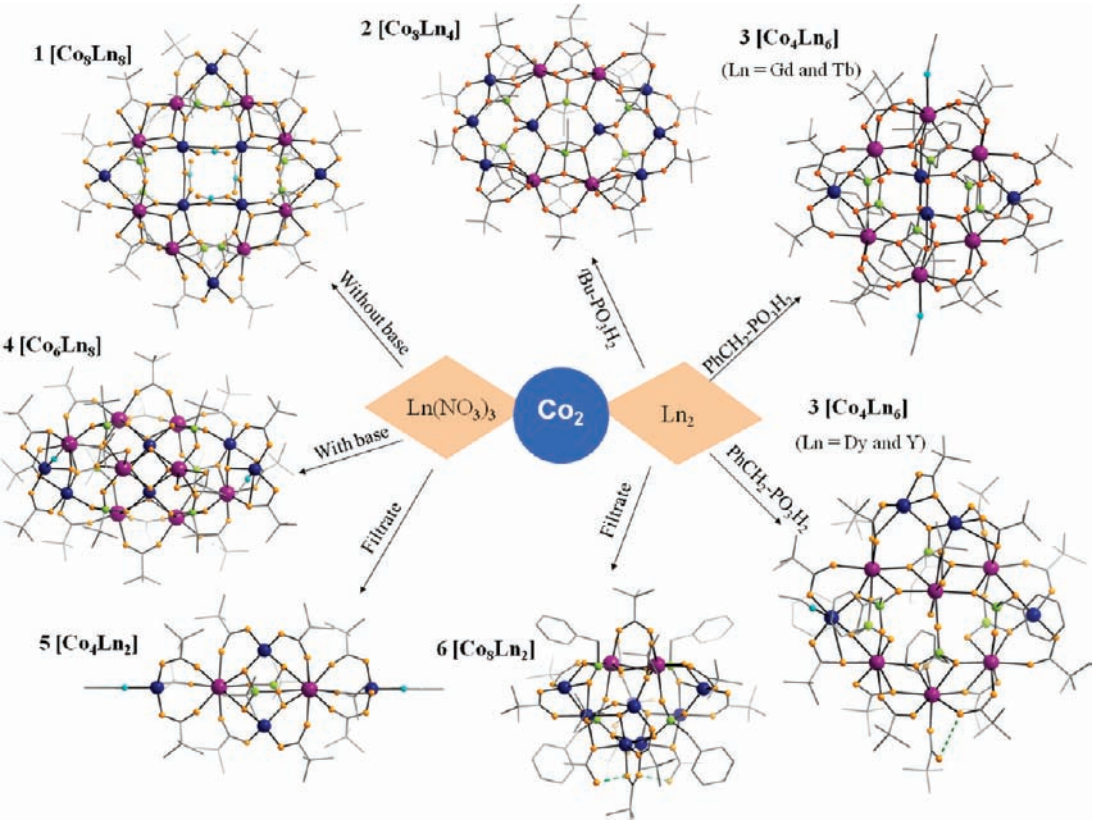

Figure 1. Synthetic procedures and resulting structures. Color codes (applied to the following figures) for the structures: Ln, purple; Co, blue; P, green; O, orange; N, cyan; C, gray.

dx.doi.org/10.1021/ja208367k | J. Am. Chem.Soc. 2012, 134, 1057−1065

lighter lanthanides, which again suggests the size of the lanthanide ions is important in influencing the reaction pathway.

If **Gd_2** is used in place of the hydrated lanthanide nitrate salts in the same reaction that gives **1Ln** complexes, $[Co^{II}_8Gd^{III}_4(O_3P^tBu)_6(O_2C^tBu)_{16}]$ **2** can be obtained. Unfortunately, this reaction does not work for heavier lanthanides. In the same conditions, if benzylphosphonic acid is used in place of *tert*-butylphosphonic acid, a third family of compounds can be obtained: $[Co^{II}_4Ln^{III}_6(O_3PCH_2Ph)_6(O_2C^tBu)_{14}(HO_2C^tBu)_x(MeCN)_y(H_2O)_z]$ **3** (for $x = z = 0$ and $y = 2$, Ln = Gd **3Gd** and Tb **3Tb**; for $x = 1$, $y = 1$, and $z = 2$, Ln = Dy **3Dy** and Y **3Y**). Although the formulas of the **3Gd** and **3Tb** are similar to those of **3Dy** and **3Y**, the structures are different (vide infra). If we use **Nd_2**, we do not obtain crystals directly from the autoclave, but crystals grow in the solutions formed in the autoclave after a few weeks. The crystals contain the compound $[Co^{II}_8Nd^{III}_2(\mu_3\text{-}OH)_2(O_3PCH_2Ph)_4(O_2C^tBu)_{12}(HO_2CMe)_2](MeCN)_6$ **6Nd**, and the gadolinium analogue **6Gd** can also be made this way.

Structural Description. We have divided the Co–Ln families of compounds into two groups, grid families involving structures **1**, **2**, **3**, and **5**, and the cage families, **4** and **6**.

Structures of the Grid Families 1, 2, 3, and 5. These are rare examples of mixed-metal grids as compared to previously reported homometallic grids.[22−25] The core of family **1** features a central nitrate-bridged $[Co_4]$ square (Figure 2), which is

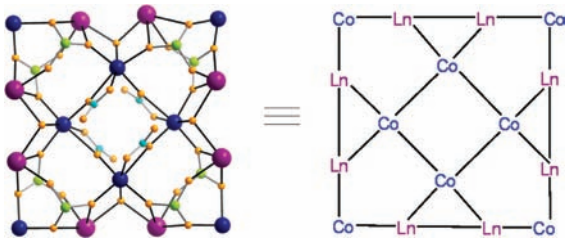

Figure 2. The $[Co_8Ln_8]$ core of **1** (left) and its rotated-[4 × 4] grid representation (right).

connected to an outer $[Ln_8]$ ring through oxygen atoms from either phosphonate or hydroxide ligands. There are also four tetrahedral cobalt(II) ions at the corners of the outer square. The structure is therefore a [4 × 4] grid with the central square rotated by ca. 45° with respect to the outer ring. If the four corner cobalt ions were removed, the 12 metal core is similar to the famous $\{Mn_{12}\}$ single-molecule magnet,[26] in which four central manganese(IV) ions are surrounded by eight manganese(III) ions, except that the central four central manganese(IV) ions are in a cubane geometry rather than a [2 × 2] square.

The second grid family features a [4 × 3] grid (Figure 3). The central row of the grid contains four four-coordinate cobalt(II)

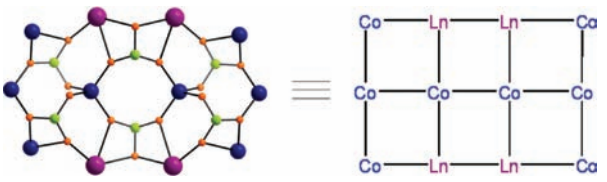

Figure 3. The $[Co_8Ln_4]$ core of **2** (left) and its [4 × 3] grid-skeleton representative (right). Note that this grid representation does not discriminate the different magnetic interactions.

ions with tetrahedral coordination geometries, while the four cobalt sites in the outer rows of the grid are five-coordinate with a geometry close to trigonal-bipyramidal ($\tau = 0.72$).[27] The relative sizes of Co and Gd lead to the grid being irregular, with the Co···Gd separations (4.0 Å) greater than the Co···Co separation (3.3 Å).

The core structure of family **3** shows the influence of the phosphonate ligands; as compared to the *tert*-butyl substitute used in families **1** and **2**, the less bulky benzyl group allows the phosphonate to bind to more metal ions. When the lanthanides are Gd or Tb, the core features a central cobalt(II) dimer that is surrounded by other metal centers due to the bridging phosphonate. If the central cobalt(II) dimer is viewed as a single node, the resulting topology of this core is a [3 × 3] grid (Figure 4).

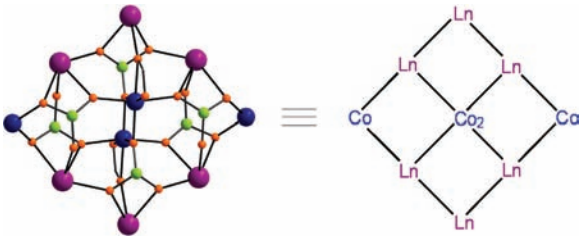

Figure 4. The $[Co_4Ln_6]$ core of **3Gd** and **3Tb** (left) and its [3 × 3] grid representation (right). Note that Co_2 represents the central cobalt(II) dimer.

Complex **3Dy** is noticeably less symmetrical than **3Tb**, with the central cobalt(II) dimer found at the edge of the grid in **3Dy** (Figure 5). There is also a change of space group from

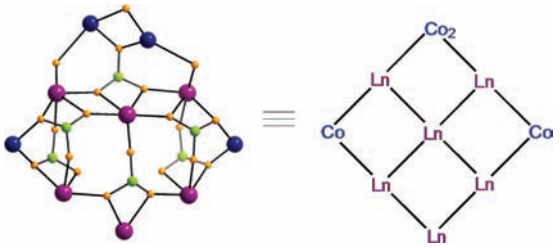

Figure 5. The $[Co_4Ln_6]$ core of **3Dy** and **3Y** (left) and its [3 × 3] grid representation (right). Note that Co_2 represents the cobalt(II) dimer.

$P2_1/n$ to $P\text{-}1$. The coordination geometries of the cobalt(II) ions differ between the two structures. In **3Tb**, two Co sites have tetrahedral geometries and two octahedral, while in **3Dy** only one cobalt site is tetrahedral and the other three are five-coordinate with a geometries best described as square-pyramidal (τ ranges from 0.3 to 0.5).[27] The metal–metal contacts vary between the structures: in **3Tb**, average contacts are Tb···Tb 4.09 Å, Co···Tb 3.85 Å, with the Co···Co contact in the dimetallic unit 3.18 Å; in **3Dy**, average contacts are Dy···Dy 3.92 Å, Co···Dy 3.72 Å, and the short Co···Co contact 3.34 Å. The phosphonates show the 4.221 and 5.222 coordination modes in **3Gd**, **3Tb**, and **3Dy**, while in **3Dy** a single example of the 3.211 mode is also found.

The **5Ln** family contains at its center a [2 × 2] grid, with cobalt and lanthanide ions at alternate corners of a rhombus (Figure 6). The Co···Ln edges of the rhombus are 3.74 Å long. The metals are bridged by two 4.221 *tert*-butylphosphonates at the center and four 2.11 pivalates on the edges. A further external cobalt site is bound to each lanthanide site by three 2.11 bridging pivalates, with a Co···Ln contact of 3.92 Å. All of the cobalt(II) sites in this structure have a tetrahedral geometry.

dx.doi.org/10.1021/ja208367k | J. Am. Chem.Soc. 2012, 134, 1057–1065

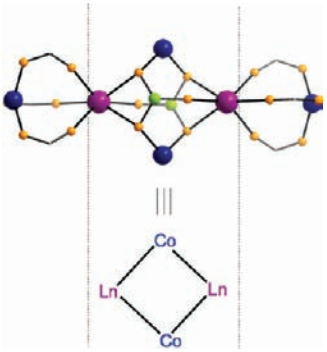

Figure 6. $[Co_4Ln_2]$ core of **5** (upper) and its central [2 × 2] grid-skeleton representative (lower).

Before considering the cage families, we note the shape of these complexes. As many proposed applications of molecular magnets involve deposition on surfaces, a good contact between the molecule and the substrate is desirable. As can be seen from Figure 7, the grid molecules are roughly flat; however,

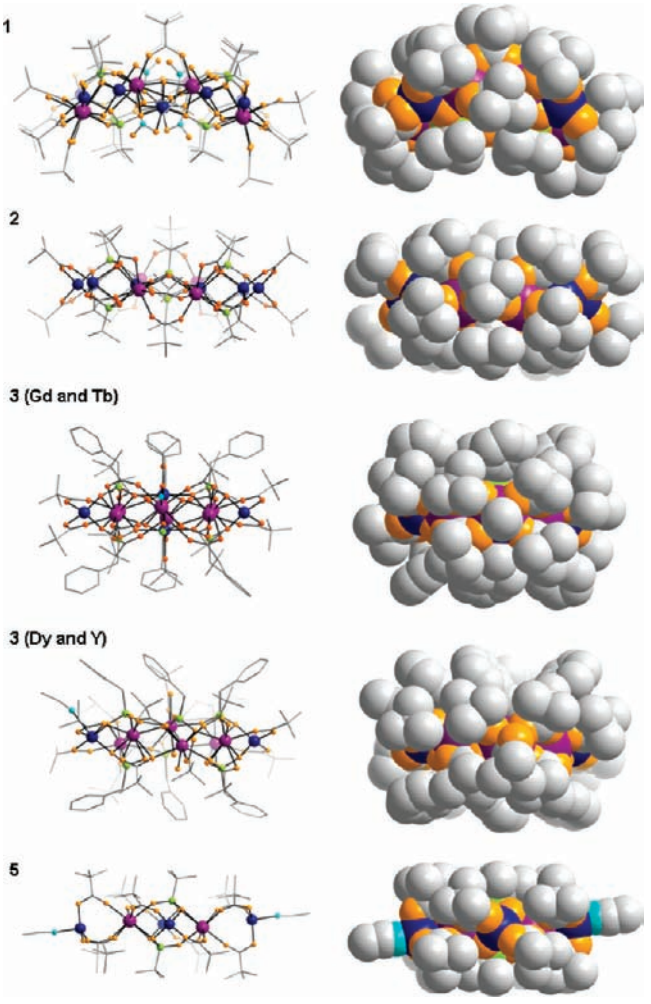

Figure 7. The ball-and-stick (left) and the space-filling (right) views of the labeled grid families.

as the numbers of the metal sites increase, the molecule becomes less planar. This is best seen from the bending of the largest [4 × 4] grid in the family **1**. This observation is consistent with other homo- and heterometallic grids. The largest grid from Thompson's group contains 20 metal centers in a [5 × 5] grid, as shown by current-imaging tunneling spectroscopy (CITS) imagery on a highly ordered graphite (HOPG) surface,[22h] and is difficult to crystallize possibly because the structure is not planar, unlike smaller grids from the Thompson group.[22]

Structures of the Cage Families 4 and 6. If base is added to the synthesis that produces family **1**, a new family of cages **4** can be obtained. The structure of this family features eight μ_3-hydroxides that form the bridge between the six cobalt and eight lanthanide centers at the core of the complexes (Figure 8a). At the center is a $[Co^{II}_2Ln^{III}_2(\mu_3\text{-}OH)_4]^{6+}$ cubane, with a larger Ln−O−Ln angle (109.4°) as compared to smaller Ln−O−Co (100.7°) and Co−O−Co angles (100.1°). This cubane is attached to one side of a $\{Co_2Ln_6O_8\}$ ring, through two μ_3-hydroxides and four 4.221 phosphonates. Two further 4.221 phosphonates bind to the under-side of this ring. There are two further cobalt centers bound to the $\{Co_2Ln_6O_8\}$ ring through μ_3-hydroxides. These cobalt sites are above the plane of the $\{Co_4Ln_6O_8\}$ ring (bottom Figure 8), folding toward the $[Co^{II}_2Ln^{III}_2(\mu_3\text{-}OH)_4]^{6+}$ cubane. All of the cobalt sites are five-coordinate with a geometry close to trigonal bipyramid (τ = 0.65)[27] with the fifth coordination site occupied by a solvent molecule. The average nearest Co···Ln, Ln···Ln, and Co···Co separations throughout the structure are about 3.50, 3.90, and 3.20 Å, respectively. The presence of so many hydroxides gives this cage an inorganic core wrapped within a strongly hydrophilic exterior consisting of *tert*-butyl groups from either pivalates or phosphonates (Figure 8b).

The core of the **6Ln** complexes contains eight cobalt and two lanthanide ions that are bridged by four 4.221 phosphonate ligands (Figure 9a). The two lanthanide ions are bridged by a μ-oxygen from a phosphonate, forming an Ln_2O_2 rhombus. The two phosphonates involved each bridge to two cobalt centers. In each case, one of these cobalt centers forms part of a $[Co_3(\mu_3\text{-}OH)]$ triangle, with these two triangles in the structure linked through two μ-oxygens from a further phosphonate. Two of the cobalt sites in each triangle have an octahedral geometry, while the third is tetrahedral. The second cobalt bound to the central phosphonates in each case has a tetrahedral coordination geometry. The average nearest Co···Ln, Ln···Ln, and Co···Co separations are ca. 3.72, 3.99, and 3.23 Å, respectively. There is a small space as indicated by the yellow spheres (Ø = 4.6 Å without eliminating the van der Waals) in Figure 9a in this $\{Co_8Ln_2\}$ core, which is surrounded by the organic ligands. Two protonated acetate ligands in the peripheral adopt a 2.20 mode bridging two adjacent cobalt(II) ions and form hydrogen bonding with the oxygen atom from nearby pivalates (O···O distance of 2.82 Å and O−H···O angle of 167°), as shown in Figure 9b. This coordination mode of acetate is also found in a $\{Ni_6Ln_6\}$ Wells−Dawson cage.[11b] We reason that the formation of the acetate is from hydrolysis of acetonitrile in solvothermal reaction; this has been observed previously.[11b,28,29]

MAGNETIC PROPERTIES

The magnetic behavior of polycrystalline samples of families **1**−**6** has been studied, and the results are summarized in Table 1. The room temperature χT values were used to calculate the average *g*-value per cobalt site, using the known ground state for each 4f-ion and the Curie constant for those ions. The calculation also assumes that any interaction between spins is insignificant at room temperature. The *g*-value should be related to the coordination geometry of the Co(II) ions, with octahedral

dx.doi.org/10.1021/ja208367k | J. Am. Chem.Soc. 2012, 134, 1057−1065

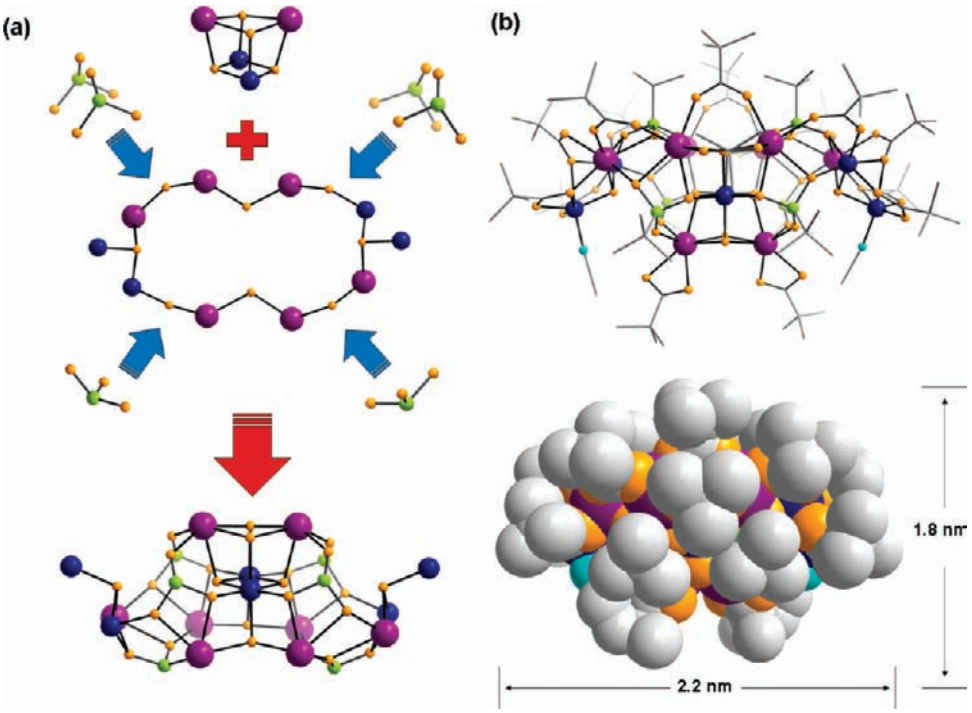

Figure 8. The subunits of the $\{Co_6Ln_8\}$ core (a) and the ball-and-stick and space-filling side views (b) of **4**.

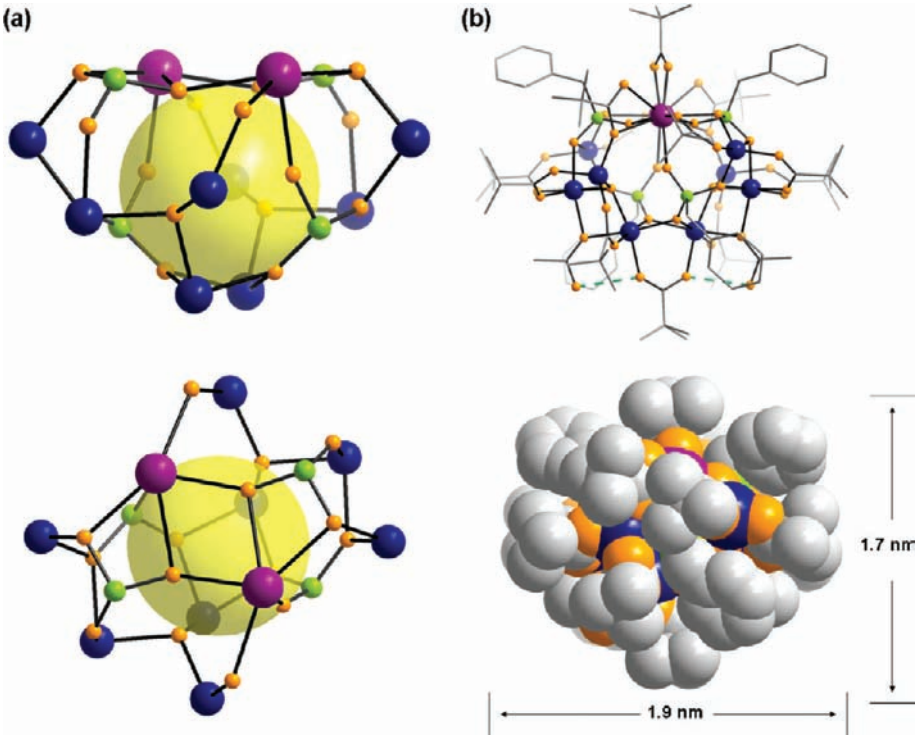

Figure 9. Side (upper) and top (lower) views of the $\{Co_8Ln_2\}$ core (a) and the ball-and-stick (upper) and space-filling (lower) side views (b) of **6**. The yellow spheres indicate the space within the cage, and the dotted green lines indicate the hydrogen bondings between the oxygen atoms.

geometries giving larger values than tetrahedral due to spin–orbit coupling. The result is inconclusive, showing a range of *g*-values for the cobalt sites in each family, which suggests that the assumption of no significant interaction is invalid. More sophisticated analysis of the magnetism of such complex structures involving ions with an orbital component of their magnetism is presently impossible.

For all compounds, the χT decreases steadily with decreasing temperature due to the spin–orbital coupling effect of the cobalt(II) ions and the lanthanide centers (gadolinium excepted) (Figures 10 and S1–S4).[12,30–35] Although in most cases the χT versus T curve is falling at 2 K, there are upward turning points observed in the case of **3Gd** and **5Gd** (Figures 10 and S3), which suggests either ferromagnetic interactions in these two compounds, or ferromagnetic

dx.doi.org/10.1021/ja208367k | *J. Am. Chem.Soc.* 2012, 134, 1057–1065

Table 1. Magnetic Data for Families 1−6

compound	obs χT at 300 K (cm^3 mol^{-1} K)	calcd average g-value for Co(II)	obs χT at 2 K (cm^3 mol^{-1} K)	obs M at 2 K and 7 T (μ_B)	$-\Delta S_m$ at 3 K and 7 T (J kg^{-1} K^{-1})
1Gd	82.7	2.29	36.1	39.2	21.4
1Tb	118.5	2.53	38.8	49.1	
1Dy	134.0	2.35	61.3	57.5	11.6
1Ho	136.1	2.51	55.4	56.0	
1Er	117.3	2.61	59.0	55.5	
1Yb	47.6	2.69	21.1	21.9	
1Y	23.0	2.48	5.5	11.0	4.5
2Gd	54.6	2.48	36.1	39.2	21.1
3Gd	61.6	2.76	79.3	46.5	23.6
3Tb	84.9	2.73	42.8	35.6	
3Dy	97.6	2.59	65.4	46.1	
3Y	12.6	2.59	8.0	10.6	
4Gd	81.9	2.59	59.0	64.1	28.6
4Tb	111.5	2.45	40.4	38.1	
4Dy	127.5	2.24	59.8	49.0	
4Ho	126.8	2.25	41.3	52.5	
4Er	112.3	2.70	46.3	48.9	
4Y	19.2	2.61	1.7	7.5	
5Gd	26.2	2.36	21.9	20.1	20.0
5Nd	13.4	2.32	4.4	9.8	
6Gd	42.4	2.66	11.4	25.1	11.8

behavior. In all cases, the value of χT is not zero at the lowest temperature measured, suggesting that paramagnetic states are still populated due to the very weak exchange involving 4f-ions.

Magnetization (M) measurements from 2 to 10 K (insets of Figures 10, S1−S4) in each case show a steady increase with increasing field (B), but do not saturate at 7 T. This feature has been widely observed in complexes containing antiferromagnetic exchange. By comparing the slopes of the M versus H plots, we can discern that those gadolinium-containing analogues in each family are steeper at lower field. In other words, they are easier magnetized, which is critical in magnetic cooling applications.

The magnetic study of yttrium analogue allows us to study the magnetic interactions between the cobalt centers in each family. The M versus B plots of **1Y**, which contains four tetrahedral and four octahedral cobalt(II) sites (Figure 2), at low temperatures (2−6 K) reach 11.0 μ_B at 7 T at 2 K (inset of Figure S1, **1Y**). This value is consistent with four uncoupled tetrahedral cobalt(II) ions (calcd 11.0 μ_B for four $S = 3/2$, $g = 2.48$ centers). Therefore, we reason that the octahedral cobalt(II) ions in the central $\{Co_4\}$ square are antiferromagnetically coupled, leading to a diamagnetic ground state for this subunit, while the remaining corner tetrahedral cobalt(II) ions behave as almost uncoupled ions in **1Y**. However, attempts to fit these data to the sum of the Brillouin functions for four $S = 3/2$ ions were not successful, suggesting significant anisotropy for the four tetrahedral cobalt(II) sites. Attempts to model the data further did not seem wise, given the assumptions made about the octahedral cobalt sites. The magnetization behavior of **3Y** is similar, again suggesting the cobalt(II) sites are uncoupled.

For **4Y**, χT falls much faster below 100 K, approaching a nearly vanished value at 2 K. Field-dependent magnetization at low temperatures (inset of Figure S2, **4Y**) shows a linear increase, indicating antiferromagnetic interactions between the

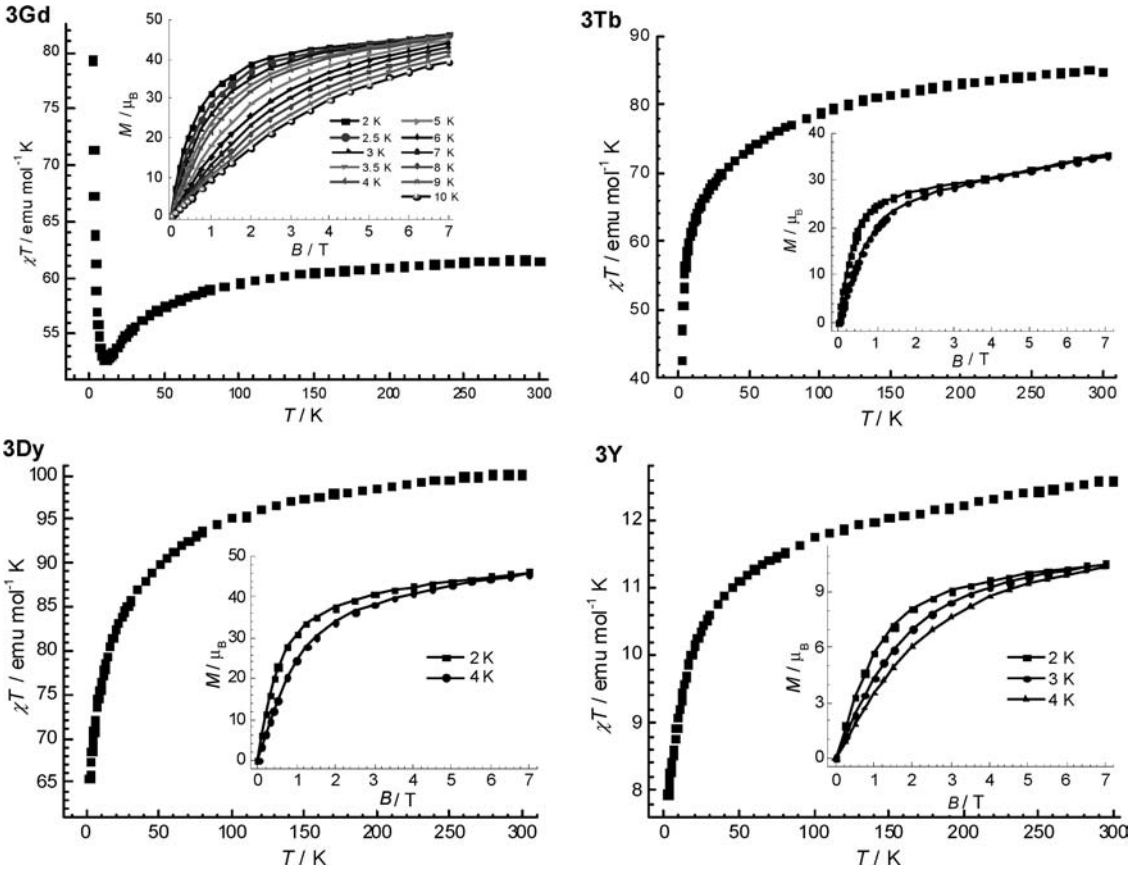

Figure 10. The χT versus T plot of family **3** under 0.1 T dc field. Inset: The field-dependent magnetization plots at indicated temperatures. Lines are visual guides.

dx.doi.org/10.1021/ja208367k | J. Am. Chem.Soc. 2012, 134, 1057−1065

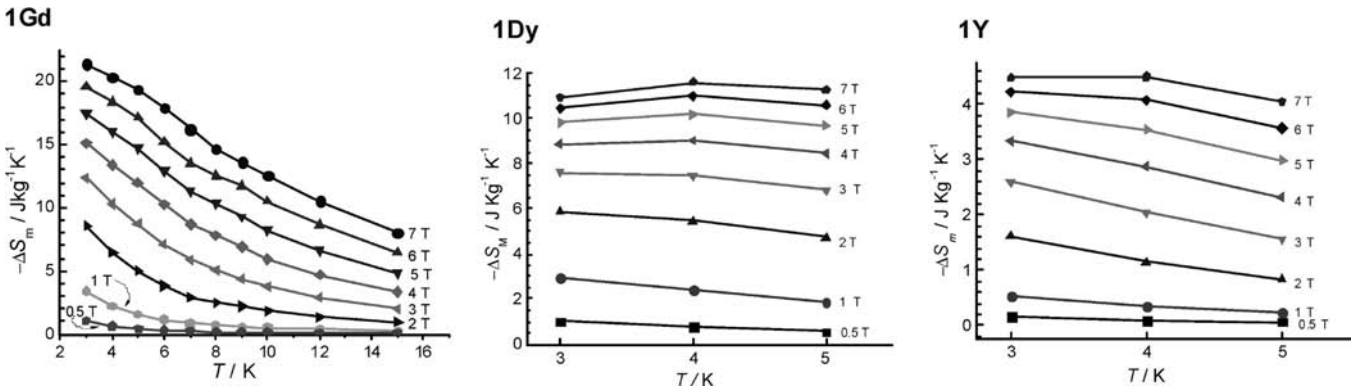

Figure 11. Experimental ΔS_m for **1Gd**, **1Dy**, and **1Y** at various fields and temperatures. Lines are guides to the eye.

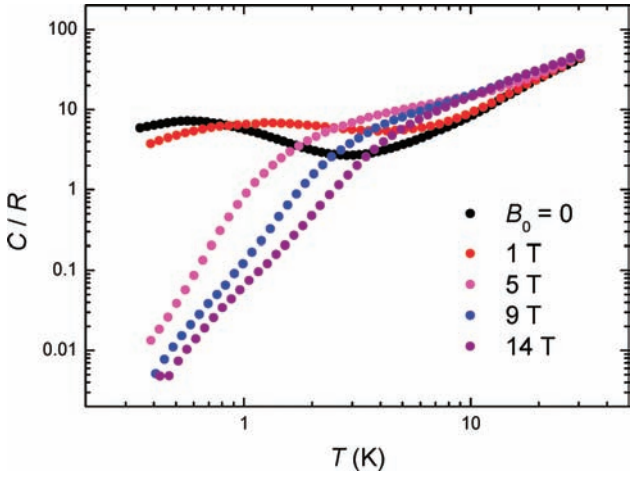

Figure 12. Experimental heat capacity C of **4Gd**, normalized to the gas constant R, at various fields and temperatures.

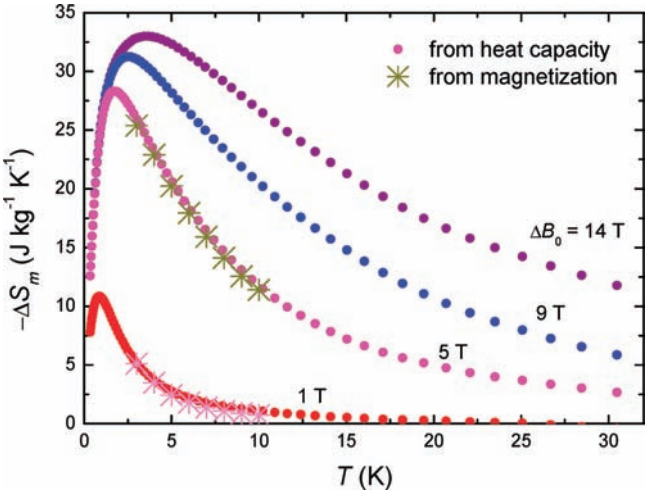

Figure 13. Experimental ΔS_m for **4Gd** at various fields and temperatures, as obtained from the heat capacity data. The ΔS_m deduced from the magnetization data is also plotted for comparison, proving the remarkable agreement between these two complementary techniques.

cobalt(II) centers and an $S = 0$ ground state. Therefore, it is reasonable to conclude that the cobalt(II) pairs in the central $\{Co_2Ln_2\}$ cubane and the $\{Co_2Ln(\mu_3\text{-OH})\}$ triangles are antiferromagnetically coupled.

Ac susceptibility studies show no slow relaxation of magnetization in any of these compounds; none of them are single-molecule magnets. To compare the MCE of the previously reported **1Gd** complex, entropy changes (ΔS_m) of **1Dy** and **1Y** have been performed according to the Maxwell equation $\Delta S_m(T)_{\Delta B} = \int [\partial M(T,B)/\partial T]_B \, dB$.[1] As expected, the resulting entropy changes of **1Dy** and **1Y** are much smaller than those of the gadolinium analogue (Figure 11). The maximum $-\Delta S_m$ of **1Dy** occurs at higher temperature (4 K), and the value (11.6 J kg^{-1} K^{-1}) is just one-half of gadolinium analogue. The tendency of $-\Delta S_m$ versus T plots of **1Y** is similar to the dysprosium analogue, but the maximum value is even lower, in accord with the lower magnetic density of **1Y**.

Entropy changes were calculated from the magnetization data for all of the gadolinium cages. For the **4Gd** complex (top Figure S5), the $-\Delta S_m$ versus T plots increase gradually from 10 to 3 K, reaching a maximum of 28.6 J kg^{-1} K^{-1} at 7 T. There is still no sign of a downturn, which means the maximum of the **4Gd** should come at a lower temperature for the investigated applied field changes. For **5Gd**, the $-\Delta S_m$ versus T plots reach a maximum of 20.0 J kg^{-1} K^{-1} (middle of Figure S5). This value is lower than that observed in **4Gd**. For **6Gd**, the maximum is 11.8 J kg^{-1} K^{-1} (bottom of Figure S5). The results show, again unsurprisingly, that the entropy change increases with the gadolinium content of the cage.

HEAT CAPACITY

To further investigate the observed largest magnetothermal effect of **4Gd**, we have performed heat capacity measurements, which represent the best experimental tool for the assessment of the MCE.[7] Figure 12 shows the dependence on temperature of the heat capacity of **4Gd**, collected for 0.35 K < T < 30 K and applied fields B_0 = 0, 1, 5, 9, and 14 T. Especially at the lowest temperature, it can be seen that the experimental curves are strongly dependent on the applied field, while in the high-temperature range, a large field-independent contribution appears that can be attributed to the lattice phonon modes of the crystal.

The entropy S of **4Gd** at the corresponding fields and temperatures (Figure S6) is then obtained from the heat capacity data by making use of the expression $S = \int C/T \, dT$. From this result, it becomes straightforward to obtain the magnetic entropy change ΔS_m for the selected field changes; these results compare well with the ΔS_m deduced from the magnetization data of **4Gd** (Figure 13).

dx.doi.org/10.1021/ja208367k | J. Am. Chem.Soc. 2012, 134, 1057−1065

The magnetic entropy change for **4Gd** reaches large values, for example, $-\Delta S_m$ = 33 J kg^{-1} K^{-1} at 4 K for the investigated field change, ΔB_0 from 14 to 0 T. The field-dependent maximum in $-\Delta S_m$ is approaching the full available entropy of **4Gd**, which corresponds to the sum of the entropy of six uncorrelated Co(II) and eight uncorrelated Gd(III) spins, that is, $6 \times R \ln(2S_{Co} + 1) + 8 \times R \ln(2S_{Gd} + 1) = 24.9R = 47.6$ J kg^{-1} K^{-1}.

CONCLUSIONS

To summarize, by using dimetallic cobalt(II) pivalate complex as a starting material reacted with a range of different lanthanide starting materials, we have obtained a range of 3d−4f mixed-metal complexes with six type of cores: $\{Co_8Ln_8\}$, $\{Co_8Ln_4\}$, $\{Co_4Ln_6\}$, $\{Co_6Ln_8\}$, $\{Co_6Ln_8\}$, $\{Co_4Ln_2\}$, and $\{Co_8Ln_2\}$. These 3d−4f heterometallic complexes show a potential capability for magnetic cooling at low temperatures. The observed entropy changes of the gadolinium derivatives are always the largest ones in one family, which is consistent with the need for a high isotropic spin. Finally, we observe that the MCE increases by increasing the relative percentage of the gadolinium content in the cluster core.

ASSOCIATED CONTENT

Supporting Information

Crystallographic information files (CIF). This material is available free of charge via the Internet at http://pubs.acs.org.

AUTHOR INFORMATION

Corresponding Author

richard.winpenny@manchester.ac.uk

ACKNOWLEDGMENTS

We are grateful for financial support provided by a Marie Curie International Incoming Fellowship (to Y.-Z.Z., EC contract no.: PIIF-GA-2008-219588), by the EPSRC (UK) and the Royal Society for a Wolfson Merit Award (to R.E.P.W.), and by the MICINN (Spain) through contract nos. MAT2009-13977-C03 and CSD2007-00010. We also thank Madeleine Helliwell for help with X-ray refinements, and Eric McInnes and David Collison for helpful discussions.

REFERENCES

(1) (a) Zimm, C.; Jastrab, A.; Sternberg, A.; Pecharsky, V.; Gschneidner, K. A. Jr.; Osborne, M.; Anderson, I. *Adv. Cryog. Eng.* **1998**, *43*, 1759. (b) Pecharsky, V.; Gschneidner, K. A. Jr. *J. Magn. Magn. Mater.* **1999**, *200*, 44. (c) Yu, B. F.; Gao, Q.; Zhang, B.; Meng, X. Z.; Chen, Z. *Int. J. Refrig.* **2003**, *26*, 622. (d) Pecharsky, V.; Gschneidner, K. A. Jr. *Int. J. Refrig.* **2006**, *29*, 1239. (e) Gschneidner, K. A. Jr.; Pecharsky, V. *Int. J. Refrig.* **2008**, *31*, 945.

(2) Warburg, E. *Ann. Phys. Chem.* **1881**, *13*, 141.

(3) (a) Sessoli, R.; Gatteschi, D.; Villain, J. *Molecular Nanomagnets*; Oxford University Press: Oxford, 2006. (b) Christou, G.; Gatteschi, D.; Hendrickson, D. N.; Sessoli, R. *MRS Bull.* **2000**, *25*, 66−71. (c) Gatteschi, D.; Sessoli, R. *Angew. Chem., Int. Ed.* **2003**, *43*, 268−297. (d) Aromí, G.; Brechin, E. K. *Struct. Bonding (Berlin)* **2006**, *122*, 1−67.

(4) (a) Evangelisti, M.; Candini, A.; Ghirri, A.; Affronte, M.; Brechin, E. K.; McInnes, E. J. L. *Appl. Phys. Lett.* **2005**, *87*, 072504. (b) Shaw, R.; Laye, R. H.; Jones, L. F.; Low, D. M.; Talbot-Eeckelaers, C.; Wei, Q.; Milios, C. J.; Teat, S.; Helliwell, M.; Raftery, J.; Evangelisti, M.; Affronte, M.; Collison, D.; Brechin, E. K.; McInnes, E. J. L. *Inorg. Chem.* **2007**, *46*, 4968.

(5) (a) Manoli, M.; Johnstone, R. D. L.; Parsons, S.; Murrie, M.; Affronte, M.; Evangelisti, M.; Brechin, E. K. *Angew. Chem., Int. Ed.* **2007**, *46*, 4456. (b) Manoli, M.; Collins, A.; Parsons, S.; Candini, A.; Evangelisti, M.; Brechin, E. K. *J. Am. Chem. Soc.* **2008**, *130*, 11129. (c) Nayak1, S.; Evangelisti, M.; Powell, A. K.; Reedijk, J. *Chem.-Eur. J.* **2010**, *43*, 12865.

(6) (a) Spichkin, Yu. I.; Zvezdin, A. K.; Gubin, S. P.; Mischenko, A. S.; Tishin, A. M. *J. Phys. D: Appl. Phys.* **2001**, *34*, 1162. (b) Zhang, X. X.; Wei, H. L.; Zhang, Z. Q.; Zhang, L. *Phys. Rev. Lett.* **2001**, *87*, 157203. (c) Schnack, J.; Schmidt, R.; Richter, J. *Phys. Rev. B* **2007**, *76*, 054413.

(7) (a) Evangelisti, M.; Candini, A.; Affronte, M.; Pasca, E.; de Jongh, L. J.; Scott, R. T. W.; Brechin, E. K. *Phys. Rev. B* **2009**, *79*, 104414. (b) Evangelisti, M.; Luis, F.; de Jongh, L. J.; Affronte, M. *J. Mater. Chem.* **2006**, *16*, 2534. (c) Evangelisti, M.; Brechin, E. K. *Dalton Trans.* **2010**, *39*, 4672.

(8) (a) Karotsis, G.; Evangelisti, M.; Dalgarno, S. J.; Brechin, E. K. *Angew. Chem., Int. Ed.* **2009**, *48*, 9928. (b) Karotsis, G.; Kennedy, S.; Teat, S. J.; Beavers, C. M.; Fowler, D. A.; Morales, J. J.; Evangelisti, M.; Dalgarno, S. J.; Brechin, E. K. *J. Am. Chem. Soc.* **2010**, *132*, 12983.

(9) Langley, S. K.; Chilton, N. F.; Moubaraki, B.; Hooper, T.; Brechin, E. K.; Evangelisti, M.; Murray, K. S. *Chem. Sci.* **2011**, *2*, 1166.

(10) Evangelisti, M.; Roubeau, O.; Palacios, E.; Camón, A.; Hooper, T. N.; Brechin, E. K.; Alonso, J. J. *Angew. Chem., Int. Ed.* **2011**, *50*, 6606.

(11) (a) Zheng, Y.-Z.; Evangelisti, M.; Winpenny, R. E. P. *Chem. Sci.* **2011**, *2*, 99. (b) Zheng, Y.-Z.; Evangelisti, M.; Winpenny, R. E. P. *Angew. Chem., Int. Ed.* **2011**, *50*, 3692. (c) Sharples, J. W.; Zheng, Y.-Z.; Tuna, F.; McInnes, E. J. L.; Collison, D. *Chem. Commun.* **2011**, *47*, 7650.

(12) (a) Benelli, C.; Gatteschi, D. *Chem. Rev.* **2002**, *102*, 2369. (b) Sorace, L.; Benelli, C.; Gatteschi, D. *Chem. Soc. Rev.* **2011**, *40*, 3092.

(13) (a) Tasiopoulos, A. J.; Wernsdorfer, W.; Moulton, B.; Zaworotko, M. J.; Christou, G. *J. Am. Chem. Soc.* **2003**, *125*, 15274. (b) Mishra, A.; Wernsdorfer, W.; Abboud, K. A.; Christou, G. *J. Am. Chem. Soc.* **2004**, *126*, 15648. (c) Stamatatos, T. C.; Teat, S. J.; Wernsdorfer, W.; Christou, G. *Angew. Chem., Int. Ed.* **2009**, *48*, 521. (d) Papatriantafyllopoulou, C.; Wernsdorfer, W.; Abboud, K. A.; Christou, G. *Inorg. Chem.* **2011**, *50*, 421.

(14) (a) Osa, S.; Kido, T.; Matsumoto, N.; Re, N.; Pochaba, A.; Mrozinski, J. *J. Am. Chem. Soc.* **2004**, *126*, 420. (b) Zaleski, C. M.; Depperman, E. C.; Kampf, J. W.; Kirk, M. L.; Pecoraro, V. L. *Angew. Chem., Int. Ed.* **2004**, *43*, 3912. (c) Mishra, A.; Wernsdorfer, W.; Parsons, S.; Christou, G.; Brechin, E. K. *Chem. Commun.* **2005**, 2086. (d) Aronica, C.; Pilet, G.; Chastanet, G.; Wernsdorfer, W.; Jacquot, J.-F.; Luneau, D. *Angew. Chem., Int. Ed.* **2006**, *45*, 4659. (e) Mori, F.; Nyui, T.; Ishida, T.; Nogami, T.; Choi, K.-Y.; Nojiri, H. *J. Am. Chem. Soc.* **2006**, *128*, 1440. (f) Mereacre, V. M.; Ako, A. M.; Clérac, R.; Wernsdorfer, W.; Filoti, G.; Bartolome, J.; Anson, C. E.; Powell, A. K. *J. Am. Chem. Soc.* **2007**, *129*, 9248. (g) Pointillart, F.; Bernot, K.; Sessoli, R.; Gatteschi, D. *Chem.-Eur. J.* **2007**, *13*, 1602. (h) Mereacre, V.; Ako, A. M.; Clerac, R.; Wernsdorfer, W.; Hewitt, I. J.; Anson, C. E.; Powell, A. K. *Chem.-Eur. J.* **2008**, *14*, 3577. (i) Akhtar, M. N.; Zheng, Y.-Z.; Lan, Y.; Mereacre, V.; Anson, C. E.; Powell, A. K. *Inorg. Chem.* **2009**, *48*, 3502. (j) Langley, S.; Moubaraki, B.; Murray, K. S. *Dalton Trans.* **2010**, *39*, 5066. (k) Mereacre, V.; Lan, Y.; Clerac, R.; Ako, A. M.; Hewitt, I. J.; Wernsdorfer, W.; Buth, G.; Anson, C. E.; Powell, A. K. *Inorg. Chem.* **2010**, *49*, 5293. (l) Liu, C.-M.; Zhang, D.-Q.; Zhu, D.-B. *Dalton Trans.* **2010**, *39*, 11325. (m) Kajiwara, T.; Nakano, M.; Takahashi, K.; Takaishi, S.; Yamashita, M. *Chem.-Eur. J.* **2011**, *17*, 196. (n) Liu, J.-L.; Guo, F.-S.; Meng, Z.-S.; Zheng, Y.-Z.; Leng, J.-D.; Tong, M.-L.; Ungur, L.; Chibotaru, L. F.; Heroux, K. J.; Hendrickson, D. N. *Chem. Sci.* **2011**, *2*, 1268.

(15) Clearfield, A. *Curr. Opin. Solid State Mater. Sci.* **1996**, *1*, 268 and references therein.

(16) (a) Khan, M. I.; Zubieta, J. *Prog. Inorg. Chem.* **1995**, *43*, 1. (b) Chandrasekhar, V.; Kingsley, S. *Angew. Chem., Int. Ed.* **2000**, *39*, 2320. (c) Tolis, E. I.; Helliwell, M.; Langley, S.; Raftery, J.; Winpenny, R. E. P. *Angew. Chem., Int. Ed.* **2003**, *42*, 3804. (d) Maheswaran, S.; Chastanet, G.; Teat, S. J.; Mallah, T.; Sessoli, R.; Wernsdorfer, W.; Winpenny, R. E. P. *Angew. Chem., Int. Ed.* **2005**, *44*, 5044. (e) Langley,

S. J.; Helliwell, M.; Sessoli, R.; Rosa, P.; Wernsdorfer, W.; Winpenny, R. E. P. *Chem. Commun.* **2005**, 5029. (f) Konar, S.; Bhuvanesh, N.; Clearfield, A. *J. Am. Chem. Soc.* **2006**, *128*, 9604. (g) Shanmugam, M.; Chastanet, G.; Mallah, T.; Sessoli, R.; Teat, S. J.; Timco, G. A.; Winpenny, R. E. P. *Chem.-Eur. J.* **2006**, *12*, 8777−8785. (h) Khanra, S.; Kloth, M.; Mansaray, H.; Muryn, C. A.; Tuna, F.; Sanũdo, E. C.; Helliwell, M.; McInnes, E. J. L.; Winpenny, R. E. P. *Angew. Chem., Int. Ed.* **2007**, *46*, 5568. (i) Ma, Y.-S.; Song, Y.; Li, Y.-Z.; Zheng, L.-M. *Inorg. Chem.* **2007**, *46*, 5459. (j) Langley, S.; Helliwell, M.; Sessoli, R.; Teat, S. J.; Winpenny, R. E. P. *Inorg. Chem.* **2008**, *47*, 497. (k) Chandrasekhar, V.; Nagarajan, L.; Clérac, R.; Ghosh, S.; Verma, S. *Inorg. Chem.* **2008**, *47*, 1067. (l) Konar, S.; Clearfield, A. *Inorg. Chem.* **2008**, *47*, 3492. (m) Konar, S.; Clearfield, A. *Inorg. Chem.* **2008**, *47*, 3489. (n) Konar, S.; Clearfield, A. *Inorg. Chem.* **2008**, *47*, 5573. (o) Murugavel, R.; Gogoi, N.; Suresh, K. G.; Lavek, S.; Verma, H. C. *Chem. Asian J.* **2009**, *4*, 923.

(17) Wang, M.; Yuan, D.-Q.; Ma, C.-B.; Yuan, M.-J.; Hu, M.-Q.; Li, N.; Chen, H.; Chen, C.-N.; Liu, Q.-T. *Dalton Trans.* **2010**, *39*, 7276.

(18) Baskar, V.; Gopal, K.; Helliwell, M.; Tuna, F.; Wernsdorfer, W.; Winpenny, R. E. P. *Dalton Trans.* **2010**, *39*, 4747.

(19) Harris notation describesthe binding mode as $[X{\cdot}Y_1Y_2...Y_n]$, where X is the overall numberof metal bound by the whole ligand, and each value of Y refers to the number of metal atoms attached to the different donoratoms. See also: Coxall, R. A.; Harris, S. G.; Henderson, D. K.; Parsons, S.; Tasker, P. A.; Winpenny, R. E. P. *J. Chem. Soc., Dalton Trans.* **2000**, 2349.

(20) Chaboussant, G.; Basler, R.; Gudel, H.-U.; Ochsenbein, S. T.; Parkin, A.; Parsons, S.; Rajaraman, G.; Sieber, A.; Smith, A. A.; Timco, G. A.; Winpenny, R. E. P. *Dalton Trans.* **2004**, 2758.

(21) (a) Reuben, J. In *Handbook on Physics and Chemistry of Rare Earths*; Gschneidner, K. A., Jr., Eyring, L., Eds.; North-Holland: Amsterdam, 1979; Vol. *4*, pp 515−552. (b) Wang, R.; Gao, F.; Jin, T. *Huaxue Tongbao* **1996**, *10*, 14−20 and references therein. (c) Wang, R.; Liu, H.; Carducci, M. D.; Jin, T.; Zheng, C.; Zheng, Z. *Inorg. Chem.* **2001**, *40*, 2743.

(22) (a) Thompson, L. K.; Matthews, C. J.; Zhao, L.; Xu, Z.; Miller, D. O.; Wilson, C.; Leech, M. A.; Howard, J. A. K.; Heath, S. L.; Whittaker, A. G.; Winpenny, R. E. P. *J. Solid State Chem.* **2001**, *159*, 308. (b) Thompson, L. K.; Matthews, C. J.; Zhao, L.; Wilson, C.; Leech, M. A.; Howard, J. A. K. *Dalton Trans.* **2001**, 2258. (c) Thompson, L. K.; Zhao, L.; Xu, Z.; Reiff, W. M. *Inorg. Chem.* **2003**, *42*, 128. (d) Zhao, L.; Xu, Z.; Grove, H.; Milway, V. A.; Dawe, L. N.; Abedin, T. S. M.; Thompson, L. K.; Kelly, T. L.; Harvey, R. G.; Miller, D. O.; Weeks, L.; Shapter, J. G.; Pope, K. J. *Inorg. Chem.* **2004**, *43*, 3812. (e) Thompson, L. K.; Waldmann, O.; Xu, Z. *Coord. Chem. Rev.* **2005**, *249*, 2677. (f) Dey, S. K.; Thompson, L. K.; Dawe, L. N. *Chem. Commun.* **2006**, 4947. (g) Milway, V. A.; Abedin, S. M. T.; Niel, V.; Kelly, T. L.; Dawe, L. N.; Dey, S. K.; Thompson, D. W.; Miller, D. O.; Alam, M. S.; Müller, P.; Thompson, L. K. *Dalton Trans.* **2006**, 2835. (h) Dey, S. K.; Abedin, T. S. M.; Dawe, L. N.; Tandon, S. S.; Collins, J. L.; Thompson, L. K.; Postnikov, A. V.; Alam, M. S.; Müller, P. *Inorg. Chem.* **2007**, *46*, 7767. (i) Dawe, L. N.; Thompson, L. K. *Angew. Chem., Int. Ed.* **2007**, *46*, 7440. (j) Niel, V.; Milway, V. A.; Dawe, L. N.; Grove, H.; Tandon, S. S.; Abedin, T. S. M.; Kelly, T. L.; Spencer, E. C.; Howard, J. A. K.; Collins, J. L.; Miller, D. O.; Thompson, L. K. *Inorg. Chem.* **2008**, *47*, 176. (k) Dawe, L. N.; Shuvaev, K. V.; Thompson, L. K. *Inorg. Chem.* **2009**, *48*, 3323 and references therein.

(23) Ruben, M.; Rojo, J.; Romero-Salguero, F. J.; Uppadine, L. H.; Lehn, J.-M. *Angew. Chem., Int. Ed.* **2004**, *43*, 3644 and references therein.

(24) Newton, G. N.; Onuki, T.; Shiga, T.; Noguchi, M.; Matsumoto, T.; Mathieson, J. S.; Nihei, M.; Nakano, M.; Cronin, L.; Oshio, H. *Angew. Chem., Int. Ed.* **2011**, *50*, 4844.

(25) (a) Dawe, L. N.; Abedin, T. S. M.; Kelly, T. L.; Thompson, L. K.; Miller, D. O.; Zhao, L.; Wilson, C.; Leech, M. A.; Howard, J. A. K. *J. Mater. Chem.* **2006**, *16*, 2645. (b) Arora, H.; Lloret, F.; Mukherjee, R. *Dalton Trans.* **2009**, 9759. (c) Wu, D.; Guo, D.; Song, Y.; Huang, W.; Duan, C.; Meng, Q.; Sato, O. *Inorg. Chem.* **2009**, *48*, 854.

(26) Sessoli, R.; Gatteschi, D.; Caneschi, A.; Novak, M. A. *Nature* **1993**, *365*, 141.

(27) Addison, A. W.; Rao, T. N.; Reedijk, J.; van Rijn, J.; Verschoor, G. C. *J. Chem. Soc., Dalton Trans.* **1984**, 1349.

(28) Belsky, A. J.; Brill, T. B. *J. Phys. Chem. A* **1999**, *103*, 3006.

(29) Breeze, B. A.; Shanmugam, M.; Tuna, F.; Winpenny, R. E. P. *Chem. Commun.* **2007**, 5185.

(30) Kahn, O. *Molecular Magnetism*; VCH: New York, 1993.

(31) Carlin, R. L. *Magnetochemistry*; Springer: Berlin, 1986.

(32) (a) Zheng, Y.-Z.; Tong, M.-L.; Zhang, W.-X.; Chen, X.-M. *Angew. Chem., Int. Ed.* **2006**, *45*, 6310. (b) Zheng, Y.-Z.; Tong, M.-L.; Zhang, W.-X.; Chen, X.-M. *Chem. Commun.* **2006**, 165. (c) Zheng, Y.-Z.; Xue, W.; Tong, M.-L.; Chen, X.-M.; Zheng, S.-L. *Inorg. Chem.* **2008**, *47*, 11202. (d) Zheng, Y.-Z.; Speldrich, M.; Schilder, H.; Chen, X.-M.; Kögerler, P. *Dalton Trans.* **2010**, *39*, 10827.

(33) Boča, R. *Coord. Chem. Rev.* **2004**, *248*, 757.

(34) Palii, A.; Tsukerblat, B.; Klokishner, S.; Dunbar, K. R.; Clemente-Juan, J. M.; Coronado, E. *Chem. Soc. Rev.* **2011**, *40*, 3130.

(35) (a) Lines, M. E. *J. Chem. Phys.* **1971**, *55*, 2977. (b) Ginsberg, A. P. *Inorg. Chim. Acta Rev.* **1971**, *5*, 45.